

## Imaging of early inflammation in low-to-moderate carotid stenosis by 18-FDG-PET

M.Angels Font<sup>1</sup>, Alex Fernandez<sup>2</sup>, Ana Carvajal<sup>1</sup>, Cristina Gamez<sup>2</sup>, Lina Badimon<sup>3</sup>, Mark Slevin<sup>3,4</sup>, Jerzy Krupinski<sup>1,3,5</sup>

<sup>1</sup>Department of Neurology, University Hospital of Bellvitge (HUB), Fundacio Idibell, Barcelona, Spain, <sup>2</sup>Institut de Diagnostica per la Imatge (IDI), University Hospital of Bellvitge (HUB), Fundacio Idibell, Barcelona, Spain, <sup>3</sup>Centro de Investigacion Cardiovascular, CSIC-ICCC, Hospital de la Santa Creu i Sant Pau, Barcelona, Spain, <sup>4</sup>School of Biology, Chemistry and Health Science, Manchester Metropolitan University, Manchester, United Kingdom, <sup>5</sup>Department of Neurology, Hospital Mutua de Terrassa, Terrassa, Spain

### TABLE OF CONTENTS

1. Abstract
2. Introduction
3. Material and methods
  - 3.1. Patient recruitment
  - 3.2. FDG-PET and CT brain scans
  - 3.3. Study interpretation and analysis
  - 3.4. Carotid specimens/histology/immunohistochemistry
  - 3.5. Statistical Methods
4. Results
  - 4.1. FDG ipsilateral uptake and plaque inflammation
  - 4.2. FDG uptakes in ipsi- and contralateral carotid arteries
5. Discussion
6. Acknowledgment
7. References

## 1. ABSTRACT

It is not clear if 18FDG-PET can be useful for detection of inflammation in low to moderate carotid stenosis. We studied 15 patients scheduled for endarterectomy with contralateral carotids with less than 50% stenosis. 18-FDG-PET was performed prior to CEA and 3 months following surgery. FDG-uptake values were calculated based on maximum standardized uptake value (SUV) and corresponding uptake ratios. We confirmed by CD68 macrophage staining that FDG accumulation corresponds to active inflammation ( $R=0.8$   $p<0.005$ ). We found significant correlation between the FDG-uptake in the carotids scheduled for CEA and contralateral carotids with low to moderate stenosis ( $R=0.9$   $p<0.001$ ). The FDG uptake ratio in the contralateral arteries remained stable on the follow-up imaging (1.15+/-0.2 vs. 1.14+/-0.1;  $R=0.7$   $p=0.006$ ). We did not find correlation between FDG uptake and symptomatic or asymptomatic patients, degree of carotid stenosis and vascular risk factors. This is a prospective, preliminary *in vivo* study demonstrating that low to moderate carotid atherosclerosis can be detected using 18-FDG-PET imaging and highlights the truly systemic nature of atherosclerosis.

## 2. INTRODUCTION

Atherosclerosis is a diffuse, chronic inflammatory disease that involves the vascular, metabolic and immune systems and leads to plaque vulnerability. These ruptured or so-called vulnerable/unstable atherosclerotic lesions are responsible for a significant proportion of cerebral ischemic strokes (1-2). Patient eligibility for carotid endarterectomy (CEA) or angioplasty has been traditionally centered on assessing the degree of luminal stenosis (3) and current definitions of plaque vulnerability are based on morphology and plaque texture estimated by ecodoppler imaging, Magnetic Resonance Imaging (MRI) or angiography (4-5). However, it is difficult to clearly define whether a plaque is stable or vulnerable by currently available techniques, although, in recent years advances in MRI have improved our ability to identify carotid plaque morphology (6). More recently, vulnerable atherosclerotic plaques have been characterized by their expression of high numbers of inflammatory cells (7-10) and *in vivo* imaging of the current metabolic, dynamic state of the plaque would help to identify those patients at highest risk of ischemic stroke (11-12). In a clinical situation, number of patients suffering from stroke or transient ischemic attack (TIA)

## 18FDG-PET imaging detects early carotid inflammation

**Table 1.** Subject characteristics

No of patients, n	15
Male, n (%)	11 (73)
Age	68 (range 53-80)
Symptomatic carotid disease, n (%)	10 (67)
Stroke, n (%)	4 (40)
TIA <sup>1</sup> , n (%)	4 (40)
Amaurosis fugax, n (%)	2 (20)
Hypertension, n (%)	11 (73)
Diabetes, n (%)	8 (53)
HbA <sub>1c</sub> , %	8.11 +/- 0.8
Fasting glucose prior to PET (mg/dL)	103 +/- 21
Hyperlipidemia, n (%)	11 (73)
Total cholesterol (mmol/l)	4.9 +/- 1
LDL (mmol/l)	2.8 +/- 0.9
HDL (mmol/l)	1.2 +/- 0.2
TG (mmol/l)	1.8 +/- 0.9
ApoA1 (mmol/l)	1.2 +/- 0.3
ApoB (mmol/l)	0.8 +/- 0.9
Smoker or exsmoker, n (%)	9 (60)
Coronary artery disease, n (%)	6 (40)
Peripheral vasculopathy, n (%)	4 (27)
History of stroke, n (%)	7 (47)
Antiplatelet therapy before CEA <sup>2</sup> , n (%)	9 (60)
RAS-b <sup>3</sup> therapy before CEA, n (%)	7 (47)
Statins therapy before CEA, n (%)	7 (47)
Antiplatelet therapy after CEA, n (%)	15 (100)
RAS-b therapy after CEA, n (%)	7 (47)
Statins therapy after CEA, n (%)	11 (73)

Abbreviations: <sup>1</sup>Transient Ischemic Attack, <sup>2</sup>Carotid Endarterectomy, <sup>3</sup>Renin Angiotensine System-blockers

present low-to-moderate carotid stenosis without other clear cause of their vascular event either cardiac or intracranial. Thus, studies of carotid wall with low-to-moderate stenosis due to atherosclerosis and identification of local foci of inflammation or increased risk of thrombosis may be very relevant.

Fluorine-18 fluorodeoxyglucose (18-FDG) accumulates in inflamed tissues and several groups have established that inflamed blood vessels and atherosclerotic lesions have increased uptake of 18-FDG (13-14). More recently, 18FDG uptake was shown to be greater in carotid plaques obtained from patients with clinical evidence of carotid plaque instability (15-16) and macrophage infiltration (17). This 18-FDG enhancement has been also demonstrated in animal models of atherosclerosis (18) and verified in human studies of patients with Takayasu's arteritis, giant cell arteritis, polymyalgia rheumatica and non-specific aortitis (19-21). Furthermore, recent studies have demonstrated the reproducibility of the studies with positron emission tomography (PET) Imaging (22) and changes in vascular FDG activity can be identified by repeat PET/CT imaging (23). As FDG uptake is transient and present only at the time of active inflammation, it may offer a powerful tool to provide early detection of inflammatory foci within the carotid artery. In this work we have examined the 18-FDG abnormal uptake in the contralateral carotid artery at larger than previously reported (22) two time-points in patients undergoing CEA with low-to-moderate grade contralateral stenosis (<50%).

### 3. MATERIALS AND METHODS

#### 3.1. Patient recruitment

We studied prospectively, 15 patients with internal carotid artery stenosis with indication for CEA (3,

5). We included asymptomatic patients and patients with history of recent stroke or TIA (<6 months) (Table 1). In each patient the diagnosis of carotid stenosis was made by duplex and confirmed by angio-MRI or X-ray angiography. All patients were seen by a stroke specialist. Every patient underwent laboratory studies, cranial and carotid MRI, and 18-FDG-PET before and after CEA (mean time of 101+/-10 days). One patient refused post CEA study. Patients were excluded if they had significant contralateral carotid stenosis (>50%) or contraindications to MRI or PET imaging. The study was approved by the hospital ethics committee. All the patients gave written informed consent.

#### 3.2. FDG-PET and CT brain scans

All patients received an integrated FDG-PET/CT using a Discovery ST scanner (General Electric Healthcare). All patients were normoglycemic at the time of the FDG-PET scan with non-diabetic patients harvesting all night, with the FDG-PET scan carried out in the morning and diabetic patients, harvesting 6h after taking their usual treatment, and having their glycemia corrected with insulin if necessary prior to PET scan (mean glycemia prior to PET was 103+/-21 mg/dL, Table 1). PET was performed with 3.71 mm slice thickness with 5 overlapping slices in 3D mode including brain and neck structures (two beds). A stiff cervical collar was worn to minimize patient movement. Approximately 370 MBq of FDG was administered intravenously as a bolus in a dark and quiet room, and static emission images were obtained 30-45 min later. Attenuation correction 4-slice CT helical scans (CTAC) were obtained at 3.71mm slice-thickness, 120 KV tube voltage and 60 mA tube current. PET images were reconstructed using the 3D iterative algorithm with Fourier rebinning and attenuation-weighted ordered subsets-expectation maximization (32 subsets; 5 iterations). PET

## 18FDG-PET imaging detects early carotid inflammation

**Table 2.** Positron Emission Tomography (PET) quantification data in studied subjects

Patient	Sex	Age (years)	Clinical Symptoms	Time from symptoms to PET scan	Time from PET scan to CEA <sup>3</sup>	Time from first to second PET	18FDG uptake ratio (ipsilateral carotid)	18FDG uptake ratio (contralateral carotid)	18FDG uptake ratio (control PET, contralateral carotid)
1	M <sup>1</sup>	53	Stroke	37 days	25	121	1.17	1.15	1.13
2	M	59	Stroke	7 days	0	99	0.97	0.98	1.06
3	F <sup>2</sup>	67	Asymptomatic	-	12	111	1.04	1.10	1.00
4	M	60	Asymptomatic-TIA <sup>4</sup> disartria	-	40	143	1.3	1.09	1.15
5	M	73	TIA	28 days	3	101	1.33	1.11	1.09
6	M	66	Amaurosis	16 days	7	110	1.20	1.03	1.11
7	M	72	Amaurosis	40 days	20	110	1.23	1.30	1.35
8	M	64	Asymptomatic	-	5	103	1.10	1.02	1.10
9	M	80	Stroke	20 days	4	96	0.91	0.88	0.95
10	M	59	Asymptomatic	-	45	-	1.37	1.35	-
11	M	65	TIA	14 days	9	126	1.76	1.65	1.26
12	F	77	TIA	76 days	48	175	1.13	1.12	1.50
13	F	76	TIA	53 days	3	91	1.15	1.20	1.08
14	M	80	Asymptomatic-Stroke	270 days	21	134	1.22	1.17	1.10
15	F	70	TIA	114 days	11	110	1.09	1.07	1.01

Time from symptoms to PET scan: 41.5 (7-114); Time from PET scan to CEA: 16.9 (0-48); Time from first to second PET scan: 116+/-22. Data presented for the ipsilateral carotid indicates the carotid scheduled for carotid endarterectomy (CEA), contralateral carotid is the carotid contralateral to the one scheduled for CEA, the control PET (second PET) is 18-FDG uptake ratio in the contralateral carotid on follow-up. <sup>1</sup>male, <sup>2</sup>female, <sup>3</sup>carotid endarterectomy, <sup>4</sup>Transient Ischemic Attack.

and CT images were automatically fused by use of automatic image registration software. Carotid plaque exact localization was later confirmed by angio-MRI.

### 3.3. Study interpretation and analysis

Two speciality-trained persons blinded to patient characteristics (age, sex, symptomatic or asymptomatic disease, vascular risk factors and treatment) jointly reviewed the FDG-PET/CT scans and confirmed plaque localization by angioMRI. A semi-quantitative assessment of FDG uptake was carried out for each patient. Two-centimetre circular regions of interest (ROI) were drawn on CT images around the area including carotids in each slice, and then transferred onto the corresponding co-registered PET image to enable FDG uptake values based on maximum standardized uptake value, known as target-to-background ratio (SUVmax in mg/dL). The analysis included a vascular region 56mm over and below the level of the carotid bifurcation, and slice-activity curves at 3mm intervals were calculated in order to visualize plaque and basal metabolism (details in Figures 3B, 4C). The uptake for each plaque was divided by the average of the normal vessel wall values to give an uptake ratio. This was done in order to normalize for interpatient variations in FDG delivery to the plaque and basal metabolism. The obtained ratio value was used for statistical analysis (Table 2).

### 3.4. Carotid specimens/histology/immunohistochemistry

Carotid specimens were excised by the vascular surgeon without damage to the luminal surface. They were immediately rinsed in 0.9% saline, snap frozen in liquid nitrogen, stored at -80°C, and later processed for histology. Specimens were transversely sectioned at 3-mm intervals. Plaque morphology was assessed immediately after surgery and later by examination of the anatomic pathology of haematoxylin and eosin stained sections. The peroxidase method was used for immunohistochemical staining (Vectastain kit, Vector). After blocking endogenous peroxidase, the sections were incubated with normal serum and then incubated at 4°C overnight with the primary monoclonal anti-CD68 antibody (1:100). Afterwards, sections were incubated for 1 hour with secondary antibody (1:200) at room temperature. The peroxidase reaction was visualised with 0.05% diaminobenzidine. Negative controls in which the primary antibody was replaced with PBS were used to test for non-specific binding (data not included). Computer-assisted planimetry was used to quantify areas of staining as described previously (18, 24). The sections were computerized as colour-encoded digitized images (Nikon DS-2Mv camera, DS-U2 image processing unit and analysing software NIKON NIS-Elements vs. 3.21). Each section was transformed to a binary image with the same defined threshold for all studied sections. Total section areas and areas of macrophage infiltration (CD68 positive) were outlined manually by comparing the computerized

## **<sup>18</sup>FDG-PET imaging detects early carotid inflammation**

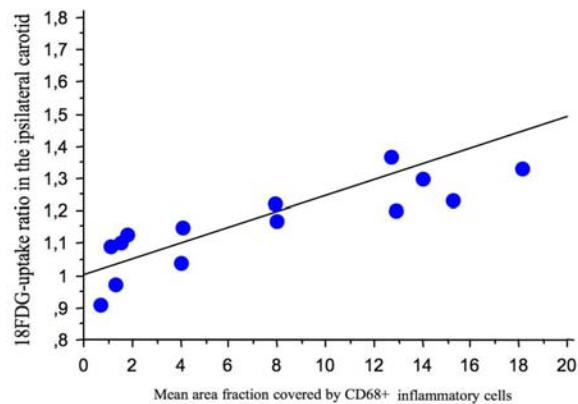


**Figure 1.** The mean area fraction covered by CD68+ inflammatory cells correlated with the degree of FDG accumulation in the atherosclerotic plaques ( $R=0.8$ ,  $p<0.005$ ).

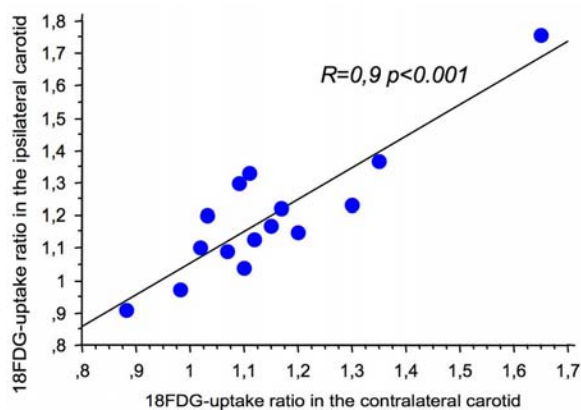


**Figure 2.** <sup>18</sup>FDG-uptake ratio in the ipsilateral carotid correlated with <sup>18</sup>FDG-uptake ratio in the contralateral asymptomatic Carotid with low-to-moderate grade of stenosis ( $R=0.9$   $p<0.001$ ).

image with images at 4x and 20x magnification. Areas of macrophage infiltration were recorded as an absolute area of staining in each slice ( $\text{mm}^2$ ). Additionally, inflammation (area fraction) was recorded as a percentage of CD68 staining. This was done in order to validate the PET FDG uptake correspondence with macrophage infiltrates.

### **3.5. Statistical methods**

Clinical data, different treatments and net <sup>18</sup>FDG accumulation rates were tested for normal distribution with K-S statistics. Correlation coefficients were assessed with Pearson or Spearman rank correlation tests for FDG uptake in the ipsilateral carotid, and contralateral areas, before and 3 months after CEA. Student's t test and Pearson correlation was used for normally distributed data. If data was not normally distributed we used non-parametric statistics, Spearman rank test for paired samples, and Mann-Whitney U tests for unpaired samples. The analyses were 2-tailed unless otherwise specified. Statistical significance was established at a P value of  $<0.05$ . Correlation was significant at a P value of  $<0.01$ .

## **4. RESULTS**

Clinical details of the 15 patients are summarized in Table 1. We included 11 men and 4 women, aged 68 (range 53-80). 10 patients had symptomatic carotid artery disease: 3 of the patients had suffered a prior ischemic stroke (PACI, superficial ACM; PACI, Deep ACM; PACI, corona radiata, respectively according to TOAST classification (25)), 4 had TIA with symptoms corresponding to the carotid scheduled for CEA, 2 had suffered amaurosis fugax and 1 patient had suffered a TIA, referring also with a previous amaurosis fugax. The remaining 5 patients were asymptomatic: 1 patient suffered a stroke (LACI) more than six months before CEA, 1 suffered a stroke in the vertebrobasilar territory, 1 had a referred transitory episode of dysarthria which prevented localization of the territory and 2 had no symptoms at all. All patients had risk factors consistent with severe atherosclerotic disease. Duplex findings were confirmed in 14 patients by angio-MRI and 1 patient by angio-MRI and X-ray angiography. Angio-MRI showed that significant stenosis was  $>90\%$  in 8 patients,  $>80\%$  in 4 patients and  $>70\%$  in 3 patients. The contralateral carotid showed  $<25\%$  stenosis in 9 patients and 25-50% in 6 patients. The mean time from the first PET scan to second one was  $116\pm 22$  days. The mean time from CEA to the second PET scan was  $101\pm 10$  days.

### **4.1. FDG ipsilateral uptake and plaque inflammation**

To confirm that in our population <sup>18</sup>FDG-PET tracks inflammation in the plaque, we quantified the mean area fraction covered by CD68+ inflammatory cells and we expressed it as a percentage of total plaque area (7.9%, range 1-18). We found a statistically significant correlation between the degree of FDG accumulation and the presence of macrophages in the atherosclerotic plaques ( $R=0.8$ ,  $p<0.005$ ) (Figure 1). This allows us to assume that contralateral carotid <sup>18</sup>FDG-uptake corresponds to active inflammation.

There was no correlation between FDG uptake and the following variables: time from symptoms to PET imaging, symptomatic (as defined by NASCET criteria (4), or recently symptomatic patients and asymptomatic patients, degree of carotid stenosis, age, gender, hs-CRP, blood pressure, serum lipids (total cholesterol, LDL-c, HDL-c, triglycerides), smoking, history of coronary artery disease, peripheral vasculopathy or prior stroke and treatment.

### **4.2. FDG uptakes in ipsi- and contralateral carotid arteries**

We found a statistically significant correlation between the degree of FDG accumulation in the ipsilateral carotids scheduled for CEA and contralateral asymptomatic carotids with low-to-moderate stenosis ( $R=0.9$   $p<0.001$ , Figure 2). The FDG uptake rates in the contralateral arteries remained stable on second exploration ( $1.15\pm 0.2$  vs.  $1.14\pm 0.1$ ;  $R=0.7$   $p=0.006$ ) with a global reduction in <sup>18</sup>FDG accumulation of 1.3% but without significant difference between the two PET explorations ( $p=0.97$ ) (Table 2, Figure 3). Patients on treatment with statins

## 18FDG-PET imaging detects early carotid inflammation

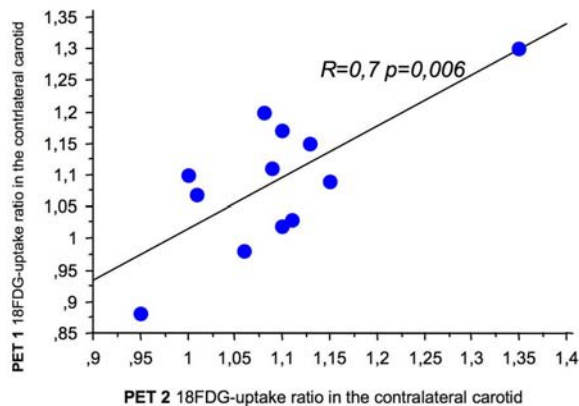


**Figure 3.** The 18FDG-uptake rates in the contralateral arteries remained stable on second exploration (1.15±0.2 vs. 1.14±0.1;  $R=0.7$   $p=0.006$ , PET 1 vs. PET 2, respectively) with a global reduction in 18FDG accumulation of 1.3% but without significant difference between the two PET explorations.

showed a tendency to present a more pronounced decrease in FDG uptake on second PET ( $p=0.05$ ). Figures 4, 5 A to C, represent CT and 18FDG-PET fused images and corresponding slice-activity curves calculated in order to represent 18FDG-uptakes. Each point corresponds to individual uptake in the studied slice (at an interval of 3mm).

## 5. DISCUSSION

In this prospective study we examined the association of bilateral carotid disease with plaque metabolic activity in patients with low-to-moderate asymptomatic contralateral stenosis. In our series, patients scheduled for CEA had a notable inflammatory response in the contralateral carotid that could be tracked by 18FDG-PET imaging. There was an important correlation in 18FDG accumulation between ipsi- and contralateral carotids. As has been recently reported (15, 17-18, 26), we have found a significant correlation between ipsilateral FDG uptake and cellular inflammatory response in the carotid plaque. The contralateral FDG uptake, if present, would therefore probably be associated with macrophage inflammatory foci in the asymptomatic artery. Importantly, contralateral 18FDG-uptake remained stable after 3 months. This may expand the 14 days window recently suggested by Rudd *et al* (27), at least, for carotids with low-to-moderate stenosis.

A recent study established that FDG-PET imaging could be used to assess the severity of inflammation in human carotid plaques (17). The authors found a significant correlation between the PET signal from carotid plaques and macrophage staining from the corresponding histology sections. This correlation was even stronger when they compared mean FDG uptake with mean percentage CD68 staining, as we have used in our study. FDG uptake did not correlate with plaque area, thickness or area of smooth muscle cell staining. Additionally, in animal

models, macrophage density, assessed by histology, correlated with non-invasive PET measurements of FDG uptake in rabbit atherosclerotic aortas. FDG uptake did not correlate with either aortic wall thickness or smooth muscle cell staining of the specimens (18, 26). Our study confirms that in our hospital-based population carotid 18FDG-uptake corresponds to inflammation in the plaque.

All previous studies using 18FDG-PET included only recent symptomatic patients with high-grade carotid stenosis or were retrospective studies in patients with cancer (28). In our study we have included symptomatic and asymptomatic patients. The symptomatic patients could be recent (<1 month) or not. Studies using 18FDG-PET and high resolution MRI suggest that we could identify the culprit lesion responsible for a cerebrovascular event by 18FDG PET (16). Authors reported 12 patients with recent TIA, 10 exhibited high FDG uptake, in 7 the uptake was seen in the lesion targeted for CEA. Two other patients showed inflamed non-stenotic lesions located in the same vascular territory and one, a lesion in the vertebral artery which could also explain the symptomatology. Contralateral asymptomatic plaques demonstrated inflammation but not to the extent of the symptomatic side. Our study, although preliminary, suggests that 18FDG-PET may detect not only recently symptomatic, aggressive plaques, but also any active, inflammatory lesion independently on the grade of stenosis or symptomatology (8). Results are in agreement with previous published studies on anatomic-pathological findings in symptomatic and asymptomatic patients. Both plaques with high and moderate degree stenosis demonstrate features of inflammation and thrombosis (29). Our study further confirms, that inflammation is truly systemic. Disappointingly, it seems difficult to assume that PET will be able to identify only the culprit lesions. We did not find correlation between FDG uptake and other vascular risk factors, although the small number of patients included in the study is an important limitation to find statistically significant differences.

In our series, the contralateral carotid stenosis was low or moderate i.e.  $\leq 50\%$  in all patients, and there was an important correlation in FDG-uptake with carotids scheduled for CEA. This suggests, that if plaque vulnerability is measured by the inflammatory response, it is independent from the grade of stenosis. Similar results were also reported in a study performed by Tang *et al.* (30) using a different technique of high-resolution ultrasmall superparamagnetic iron-oxide (USPIO) enhanced MRI in 20 patients with symptomatic carotid stenosis scheduled for CEA. USPIO is taken up by activated macrophages and allows the direct visualization of macrophage infiltration of carotid atheroma *in vivo* (31). Despite a mean carotid stenosis of 46%, 95% of asymptomatic plaques demonstrated USPIO uptake, suggesting a bilateral, inflammatory burden within their carotid atheromas. We know from studies of coronary arteries that plaque rupture occurs at low degrees of narrowing and the degree of narrowing poorly predicts clinical events (32). Approximately 40% to 50% of coronary rupture sites show  $<50\%$  diameter stenosis (33), and the same may be true in

## 18FDG-PET imaging detects early carotid inflammation

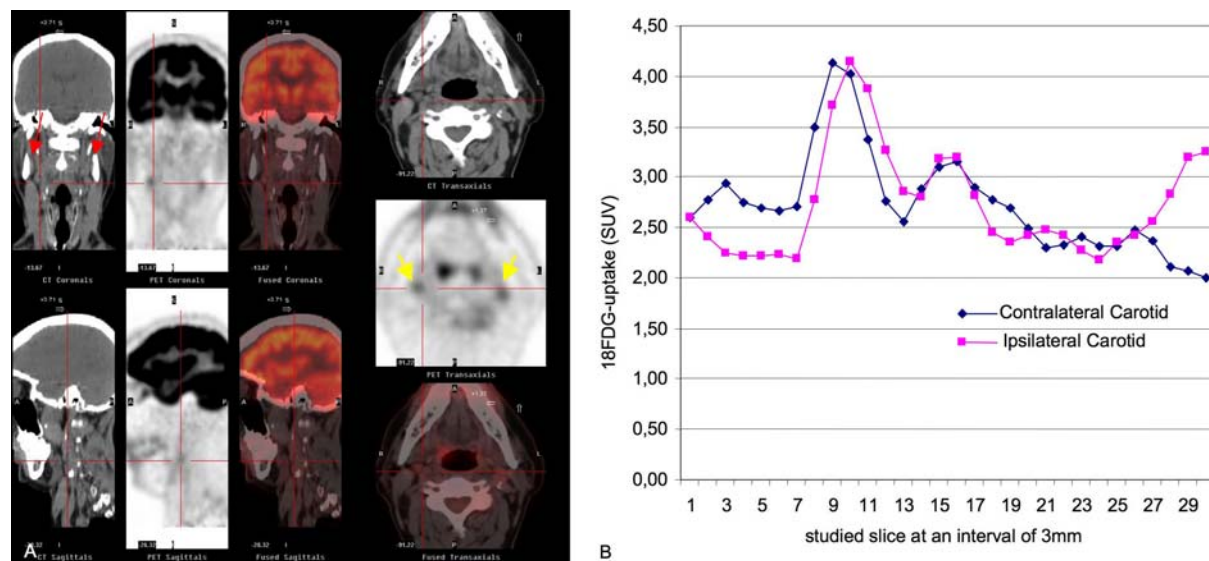


**Figure 4.** A. High resolution CT, 18FDG PET and fused images; coronal, sagittal and transaxial slices taken from patient number 11, a man of 65 years, with dyslipidemia treated with statins and family history of coronary artery disease, diagnosed with left carotid territory stroke who was referred for aphasia and right hemiparesia and several left amaurosis fugax episodes during the last three months. Ecodoppler and angio-MRI showed calcified diffuse plaques with preocclusive left internal carotid stenosis, 50% right internal carotid stenosis and occlusion of right vertebral artery. CT demonstrated several calcified areas (red arrows). PET showed high 18FDG uptake areas on both carotid arteries (yellow arrows). B. Slice-activity curves were calculated in order to represent 18FDG-uptakes. Each point corresponds to individual uptake in the studied slice (at an interval of 3mm). Points 1 to 14 correspond to internal carotid artery. Point 15 corresponds to carotid bifurcation. Points 16 to 30 correspond to the common carotid artery. Slice-activity curves show an increased FDG uptake ratio at the internal carotid artery and bifurcation on both arteries (ipsilateral carotid scheduled to CE showing a 1.76 ratio and contralateral carotid a 1.65 ratio).

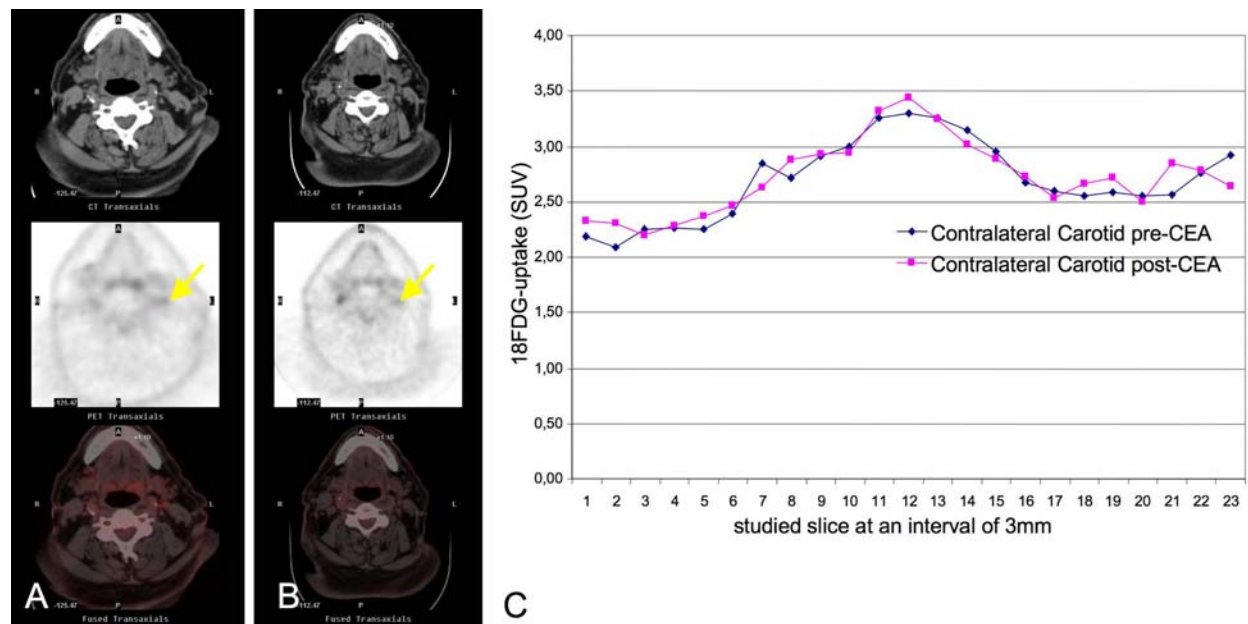


**Figure 5.** A. High resolution CT, 18FDG PET and fused images; transaxial slices taken from patient number 7, a 72 year old man with history of hypertension, diabetes and dyslipidemia taking aspirin, RAS-b and statins, who suffered a right amaurosis fugax. AngioMRI showed a 90% right stenosis and 25% left stenosis in carotid bifurcation. Yellow arrow highlights FDG uptake in the left internal carotid artery before (A) and after (B) CEA. C. In this patient there was increased 18FDG-uptake in the bifurcation area of the contralateral carotid to the one scheduled for CEA (ratio 1.30). 18FDG-uptake remained stable on second exploration (ratio 1.35).

carotid disease (34). It has recently been shown that risk of plaque rupture, and, therefore, risk of a downstream embolic event, is determined more by plaque composition than plaque size or degree of stenosis (35). But neither the ACST nor ACAS trials were able to determine whether asymptomatic patients with 50 to 69% stenosis would benefit from surgical intervention or more aggressive medical treatment (36). Therefore, the role of surveillance of the contralateral carotid artery remains unclear. A prospective study correlating future ischemic events with inflammatory plaque activity will be necessary to confirm this hypothesis. In our series, the contralateral carotids remained asymptomatic, although, patients were not screened for silent infarcts at 3 months.

In our consecutive PET scans, the same pattern of uptake seen in the first study appears in the second one at mean time of over 3 months. Only two patients showed a decrease in FDG uptake and one patient showed high FDG-uptake in a plaque that was previously silent. Rudd *et al* (22, 27) tested the near-term reproducibility of 18FDG PET imaging of atherosclerosis in 11 and 19 patients with FDG-PET/TC twice, 14 days apart and assessed interobserver and intraobserver agreement and interscan variability concluding spontaneous change in plaque FDG uptake is low and 18FDG PET is highly reproducible.

Patients on treatment with statins showed a tendency to present a more pronounced decrease in FDG uptake on second PET ( $p=0.05$ ). Only seven patients were on statins before they presented with stroke symptoms or they PET scans were performed. Following PET-imaging, 4 patients did not receive statins, one was an asymptomatic patient with normal lipidic profile, one was a symptomatic patient with LDL levels of 1.5mmol/L and 2 patients withdraw the treatment. However, the heterogeneity of doses and timing prompts to perform further studies to confirm this tendency.

We believe there is a need for new adjuncts to risk-stratify patients. Patient symptomatology and degree of luminal narrowing, which have been previously used as clinical grounds for surgical intervention, could be no longer appropriate to be considered solely for decision making. The finding of corresponding activity in the contralateral plaque is a finding that highlights the truly systemic nature of vulnerable and inflammatory atheroma. One of the limitations of the study is that it is a hospital-based cohort of patients with both symptomatic and asymptomatic carotid disease. Truly asymptomatic patients would certainly be an interesting group for future PET studies with MRI assesment of new silent brain lesions and follow-up study of any cardiovascular events. New studies should confirm the effect of statins on plaque inflammatory activity. Whether identification of an inflammatory phase in atherosclerotic carotid disease with PET will help in stratify risk and patient selection for more detailed cardiovascluar risk screening and early treatment will require further studies.

## 6. AKNOWLEDGEMENTS

This work was supported by grants: SAF 2006-07681 from the Ministerio de Educación y Ciencia (MEC).

## 7. REFERENCES

1. Naghavi M, P. Libby, E. Falk, S. W. Casscells, S. Litovsky, J. Rumberger, J. J. Badimon, C. Stefanadis, P. Moreno, G. Pasterkamp, Z. Fayad, P. H. Stone, S. Waxman, P. Raggi, M. Madjid, A. Zarrabi, A. Burke, C. Yuan, P. J. Fitzgerald, D. S. Siscovick, C. L. de Korte, M. Aikawa, K. E. Airaksinen, G. Assmann, C. R. Becker, J. H. Chesebro, A. Farb, Z. S. Galis, C. Jackson, I. K. Jang, W. Koenig, R. A. Lodder, K. March, J. Demirovic, M. Navab, S. G. Priori, M. D. Rekhter, R. Bahr, S. M. Grundy, R. Mehran, A. Colombo, E. Boerwinkle, C. Ballantyne, W. Insull, Jr., R. S. Schwartz, R. Vogel, P.W. Serruys, G. K. Hansson, D. P. Faxon, S. Kaul, H. Drexler, P. Greenland, J. E. Muller, R. Virmani, P. M. Ridker, D. P. Zipes, P. K. Shah, J. T. Willerson: From vulnerable plaque to vulnerable patient: A call for new definitions and risk assessment strategies: Part II. *Circulation* 108,1772-1778 (2003)
2. Spagnoli LG, A. Mauriello, G. Sangiorgi, S. Fratoni, E. Bonanno, R.S. Schwartz, D. G. Piepgras, R. Pistolese, A. Ippoliti, D. R. Holmes, Jr: Extracranial thrombotically active carotid plaque as a risk factor for ischemic stroke. *Jama* 292,1845-1852 (2004)
3. Rubio F, S. Martinez-Yelamos, P. Cardona, J. Krupinski: Carotid endarterectomy: Is it still a gold standard? *Cerebrovasc Dis* 20, Suppl 2:119-122 (2005)
4. Streifler JY, M. Eliasziw, A. J. Fox, O. R. Benavente, V. C. Hachinski, G. G. Ferguson, H. J. Barnett: Angiographic detection of carotid plaque ulceration. Comparison with surgical observations in a multicenter study. North american symptomatic carotid endarterectomy trial. *Stroke* 25,1130-1132 (1994)
5. Baroncini LA, A. P. Filho, S. G. Ramos, A. R. Martins, L.O. Murta, Jr: Histological composition and progression of carotid plaque. *Thromb J* 5, 4 (2007)
6. Yuan C, L. M. Mitsumori, K. W. Beach, K. R. Maravilla: Carotid atherosclerotic plaque: Noninvasive MRI characterization and identification of vulnerable lesions. *Radiology* 221, 285-299 (2001)
7. Libby P, Y. J. Geng, G. K. Sukhova, D. I. Simon, R. T. Lee: Molecular determinants of atherosclerotic plaque vulnerability. *Ann N Y Acad Sci* 811,134-142 (1997)
8. Krupinski J, M. M. Turu, J. Martinez-Gonzalez, A. Carvajal, J. O. Juan-Babot, E. Iborra, M. Slevin, F. Rubio, L. Badimon: Endogenous expression of c-reactive protein is increased in active (ulcerated noncomplicated) human carotid artery plaques. *Stroke* 37, 1200-1204 (2006)
9. Krupinski J, E. Catena, M. Miguel, P. Domenech, R. Vila, S. Morchon, F. Rubio, M. Cairols, M. Slevin, L.

## **<sup>18</sup>F-DG-PET imaging detects early carotid inflammation**

- Badimon: D-dimer local expression is increased in symptomatic patients undergoing carotid endarterectomy. *Int J Cardiol* 116, 174-179 (2007)
10. Turu MM, J. Krupinski, E. Catena, A. Rosell, J. Montaner, F. Rubio, J. Alvarez-Sabin, M. Cairols, L. Badimon: Intraplaque MMP-8 levels are increased in asymptomatic patients with carotid plaque progression on ultrasound. *Atherosclerosis* 187, 161-169 (2006)
11. Davies JR, J. H. Rudd, P. L. Weissberg: Molecular and metabolic imaging of atherosclerosis. *J Nucl Med* 45, 1898-1907 (2004)
12. Nighoghossian N, L. Derex, P. Douek: The vulnerable carotid artery plaque: Current imaging methods and new perspectives. *Stroke* 36, 2764-2772 (2005)
13. Lederman RJ, R. R. Raylman, S. J. Fisher, P. V. Kison, H. San, E. G. Nabel, R. L. Wahl: Detection of atherosclerosis using a novel positron-sensitive probe and 18-fluorodeoxyglucose (FDG). *Nucl Med Commun* 22, 747-753 (2001)
14. Tatsumi M, C. Cohade, Y. Nakamoto, R. L. Wahl: Fluorodeoxyglucose uptake in the aortic wall at PET/CT: Possible finding for active atherosclerosis. *Radiology* 229, 831-837 (2003)
15. Rudd JH, E. A. Warburton, T. D. Fryer, H. A. Jones, J. C. Clark, N. Antoun, P. Johnstrom, A. P. Davenport, P. J. Kirkpatrick, B. N. Arch, J. D. Pickard, P. L. Weissberg: Imaging atherosclerotic plaque inflammation with (18F)-fluorodeoxyglucose positron emission tomography. *Circulation* 105, 2708-2711 (2002)
16. Davies JR, J. H. Rudd, T. D. Fryer, M. J. Graves, J. C. Clark, P. J. Kirkpatrick, J. H. Gillard, E. A. Warburton, P. L. Weissberg: Identification of culprit lesions after transient ischemic attack by combined 18F Fluorodeoxyglucose Positron-Emission Tomography and High-resolution Magnetic Resonance Imaging. *Stroke* 36, 2642-2647 (2005)
17. Tawakol A, R. Q. Migrino, G. G. Bashian, S. Bedri, D. Vermynen, R. C. Cury, D. Yates, G. M. LaMuraglia, K. Furie, S. Houser, H. Gewirtz, J. E. Muller, T. J. Brady, A. J. Fischman: *In vivo* 18F-Fluorodeoxyglucose Positron Emission Tomography Imaging provides a noninvasive measure of carotid plaque inflammation in patients. *J Am Coll Cardiol* 48, 1818-1824 (2006)
18. Tawakol A, R. Q. Migrino, U. Hoffmann, S. Abbara, S. Houser, H. Gewirtz, J. E. Muller, T. J. Brady, A. J. Fischman: Noninvasive *in vivo* measurement of vascular inflammation with F-18 Fluorodeoxyglucose Positron Emission Tomography. *J Nucl Cardiol* 12, 294-301 (2005)
19. Hara M, P. C. Goodman, R. A. Leder: FDG-PET finding in early-phase Takayasu arteritis. *J Comput Assist Tomogr* 23, 16-18 (1999)
20. Blockmans D, A. Maes, S. Stroobants, J. Nuyts, G. Bormans, D. Knockaert, H. Bobbaers, L. Mortelmans: New arguments for a vasculitic nature of polymyalgia rheumatica using positron emission tomography. *Rheumatology (Oxford)* 38, 444-447 (1999)
21. Meller J, F. Strutz, U. Siefker, A. Scheel, C. O. Sahlmann, K. Lehmann, M. Conrad, R. Vosschenrich: Early diagnosis and follow-up of aortitis with ((18)F)FDG PET and MRI. *Eur J Nucl Med Mol Imaging* 30, 730-736 (2003)
22. Rudd JH, K. S. Myers, S. Bansilal, J. Machac, A. Rafique, M. Farkouh, V. Fuster, Z. A. Fayad: (18)Fluorodeoxyglucose Positron Emission Tomography imaging of atherosclerotic plaque inflammation is highly reproducible: Implications for atherosclerosis therapy trials. *J Am Coll Cardiol* 50, 892-896 (2007)
23. Ben-Haim S, E. Kupzov, A. Tamir, A. Frenkel, O. Israel: Changing patterns of abnormal vascular wall F-18 Fluorodeoxyglucose uptake on follow-up PET/CT studies. *J Nucl Cardiol* 13, 791-800 (2006)
24. Jander S, M. Sitzer, R. Schumann, M. Schroeter, M. Siebler, H. Steinmetz, G. Stoll: Inflammation in high-grade carotid stenosis: A possible role for macrophages and T cells in plaque destabilization. *Stroke* 29, 1625-1630 (1998)
25. Adams HP, Jr., B. H. Bendixen, L. J. Kappelle, J. Biller, B. B. Love, D. L. Gordon, E. E. Marsh, 3<sup>rd</sup>: Classification of subtype of acute ischemic stroke. Definitions for use in a multicenter clinical trial. Toast. Trial of org 10172 in acute stroke treatment. *Stroke* 24, 35-41 (1993)
26. Ogawa M, S. Shino, T. Mukai, D. Asano, N. Teramoto, H. Watabe, N. Kudomi, M. Shiomi, Y. Magata, H. Iida, H. Saji: (18)F-FDG accumulation in atherosclerotic plaques: Immunohistochemical and PET imaging study. *J Nucl Med*, 45 1245-1250 (2004)
27. Rudd J, K. Myers, S. Bansilal, J. Machac, C. Pinto, C. Tong, A. Rafique, R. Hargeaves, M. Farkouh, V. Fuster, Z. Fayad: Atherosclerosis inflammation imaging with 18FDG PET: carotid, iliac, and femoral uptake reproducibility, quantification methods, and recommendations. *J Nucl Med* 49, 871-878 (2008)
28. Tahara N, H. Kai, M. Ishibashi, H. Nakaura, H. Kaida, K. Baba, N. Hayabuchi, T. Imaizumi: Simvastatin attenuates plaque inflammation: Evaluation by fluorodeoxyglucose positron emission tomography. *J Am Coll Cardiol* 48, 1825-1831 (2006)
29. Luque A, P. Cardona, M. A. Font, A. Carvajal, M. Slevin, E. Iborra, F. Rubio, L. Badimon, J. Krupinski: Overexpression of hypoxia/inflammatory markers in atherosclerotic carotid plaques with low to moderate stenosis. *Frontiers in Bioscience* 13, 6483-6490 (2008)
30. Tang T, S. P. Howarth, S. R. Miller, R. Trivedi, M. J. Graves, J. U. King-Im, Z. Y. Li, A. P. Brown, P. J. Kirkpatrick, M. E. Gaunt, J. H. Gillard: Assessment of



## **<sup>18</sup>FDG-PET imaging detects early carotid inflammation**

inflammatory burden contralateral to the symptomatic carotid stenosis using high-resolution ultrasmall, superparamagnetic iron oxide-enhanced MRI. *Stroke* 37,2266-2270 (2006)

31. Trivedi R, J. U-King-Im, J. Gillard: Accumulation of ultrasmall superparamagnetic particles of iron oxide in human atherosclerotic plaque. *Circulation* 108, e140; author reply (2003)

32. Falk E: Pathogenesis of atherosclerosis. *J Am Coll Cardiol* 47, C7-12 (2006)

33. Falk E, P. K. Shah, V. Fuster: Coronary plaque disruption. *Circulation* 92, 657-671 (1995)

34. Benes V, D. Netuka, V. Mandys, M. Vrabec, M. Mohapl, V. Benes, Jr., F. Kramar: Comparison between degree of carotid stenosis observed at angiography and in histological examination. *Acta Neurochir (Wien)* 146, 671-677 (2004)

35. Virmani R, F. D. Kolodgie, A. P. Burke, A. Farb, S. M. Schwartz: Lessons from sudden coronary death: A comprehensive morphological classification scheme for atherosclerotic lesions. *Arterioscler Thromb Vasc Biol* 20, 1262-1275 (2000)

36. Rothwell PM, M. Eliasziw, S. A. Gutnikov, C. P. Warlow, H. J. Barnett: Endarterectomy for symptomatic carotid stenosis in relation to clinical subgroups and timing of surgery. *Lancet* 363, 915-924 (2004)

**Key Words:** <sup>18</sup>FDG-PET, Atherosclerosis, Carotid Disease, Inflammation

**Send correspondence to:** Jerzy Krupinski, Department of Neurology, Hospital Mutua de Terrassa, 08221 TERRASSA, Spain. Tel. 34-93-736 50 50: Fax.34-93-786 03 00 E-mail: jkrupinski@mutuaterrassa.es